

# New constraints on the up-quark valence distribution in the proton

Ritu Aggarwal,<sup>1,\*</sup> Michiel Botje,<sup>2,†</sup> Allen Caldwell,<sup>3,‡</sup> Francesca Capel,<sup>3,§</sup> and Oliver Schulz<sup>3,¶</sup>

<sup>1</sup>*USAR, Guru Gobind Singh Indraprastha University, Delhi, India*

<sup>2</sup>*Nikhef, Amsterdam, The Netherlands*

<sup>3</sup>*Max-Planck-Institut für Physik, München, Germany*

(Dated: April 7, 2023)

The high- $x$  data from the ZEUS Collaboration are used to extract parton density distributions of the proton deep in the perturbative regime of QCD. The data primarily constrain the up-quark valence distribution and new results are presented on its  $x$ -dependence as well as on the momentum carried by the up-quark. The results were obtained using Bayesian analysis methods which can serve as a model for future parton density extractions.

## INTRODUCTION

The inner structure of hadrons continues to be a subject of intense interest, with many teams pursuing quantitative studies [1–10]. Although theoretically motivated expectations exist for some aspects of the structure, precise theoretical calculations remain challenging (see, e.g., [11]) so that the quantitative behavior is effectively determined from data. The large- $x$  behavior of parton distributions in the proton has received increased interest in recent years [12, 13] and deviations from the expectations from the spectator counting rules of Brodsky and Farrar [14] are a focus of attention.

Our work is based on the high- $x$   $e^\pm p$  scattering data from the ZEUS Collaboration [15, 16] which is unique in providing measurements up to  $x = 1$  in the high  $Q^2$  regime. The data are in a kinematic region where the perturbative QCD evolution equations [17–21] are valid so that a conceptually clean analysis can be performed. Our results can furthermore serve as inputs for more global analyses [22–24]. Novel techniques were developed to carry out the present analysis [25].

The  $e^\pm p$  cross section as  $x \rightarrow 1$  is dominantly from scattering off the two up and one down valence quarks. Here the contribution from the up quarks is about one order of magnitude larger than that from down-quarks because the up quark electric charge is twice that of the down quark. We therefore focus on results on the valence up-quark distribution and report, in particular, on its power-law behavior as  $x \rightarrow 1$ . We also extract the total momentum carried by the valence up- and down-quark distributions, as well as that of the gluon distribution. These results are compared to the well-known expectations that, at asymptotically high energies, the gluons and quarks should carry approximately the same momentum (see, e.g., [26]).

The kinematics of inclusive  $e^\pm p$  scattering events are defined from the four-momenta  $p$  of the incoming proton and  $k$  ( $k'$ ) of the incoming (scattered) lepton. From these are computed the scaling variables  $Q^2 = -q^2 = -(k - k')^2$  and  $x = Q^2/(2p \cdot q)$ , and events are typically accumulated in bins of  $x$  and  $Q^2$ . The ZEUS data

used in this analysis cover the range  $0.03 \leq x \leq 1$  and  $650 \leq Q^2 \leq 20000 \text{ GeV}^2$ .

Scattering at large values of  $Q^2$  probes the proton at short (transverse) distance scales, with  $Q = 1 \text{ GeV}$  corresponding approximately to a scale of  $0.2 \text{ fm}$ . In a frame where the proton has very large momentum the Bjorken- $x$  variable has an intuitive interpretation as the fractional momentum carried by the struck parton (quark  $q$ , anti-quark  $\bar{q}$  or gluon  $g$ ) in the scattering process.

## ANALYSIS PROCEDURE

The analysis was done in a forward modeling approach where the  $e^\pm p$  cross-sections are computed from the parton distributions and, after correction for radiative and detector effects, used to predict the event numbers in the experimental set of  $x$ - $Q^2$  bins. These predictions are then compared to the measured number of events in a Bayesian analysis of the data.

To compute the cross-sections, we parameterize a set of quark, antiquark and gluon distributions  $x f_i(x)$  at a fixed value of  $Q_0^2 = 100 \text{ GeV}^2$ , with free parameters to be determined from the data. Here  $f_i(x)$  is the number density of partons of type  $i$ , and  $x f_i(x)$  is the fractional momentum density of these partons.

The QCDNUM [27] program is used to evolve these distributions to larger values of  $Q^2$  in the  $\overline{\text{MS}}$ -scheme at NNLO in perturbative QCD [28–37]. Because the data, and  $Q_0^2$ , are well above (below) bottom (top) quark mass thresholds, the evolution is carried out with 5 active quark flavors  $i = (u, d, s, c, b)$ .

In the analysis we impose the momentum sum rule and the valence quark counting rules. The momentum sum rule states that the fractional momenta of all partons in the proton add-up to unity:

$$\sum_i \int_0^1 x f_i(x) dx = \sum_i \Delta_i = 1. \quad (1)$$

We introduce here the notation  $\Delta_i$  for the total momentum fraction carried by the parton species  $i$ .

The quark counting rules fix the net number of quarks in the proton so that its quantum numbers are conserved:

$$\int_0^1 [q_i(x) - \bar{q}_i(x)] dx = \begin{cases} 2 & \text{for } i = u, \\ 1 & \text{for } i = d, \\ 0 & \text{for } i = s, c, b. \end{cases} \quad (2)$$

Here and in the following we use the notation  $q$ ,  $\bar{q}$  and  $g$  to denote quark, antiquark and gluon densities.

It is important to point out that the QCD evolution equations guarantee that sum rules which are imposed at the starting scale  $Q_0^2$  will be satisfied at all scales.

## PARAMETRIZATIONS

To parameterize the quark densities it is convenient to write them as valence ( $q^v$ ) and sea ( $q^s$ ) distributions,

$$q + \bar{q} = (q - \bar{q}) + 2\bar{q} = q^v + q^s.$$

We parameterize the valence momentum distributions as

$$xq_i^v(x, Q_0^2) = \begin{cases} A_i x^{\lambda_i} (1-x)^{K_i} & \text{for } i = u, d \\ 0 & \text{otherwise,} \end{cases} \quad (3)$$

where  $A_i$ ,  $\lambda_i$  and  $K_i$  are to be determined from the data. Replacing  $\lambda_i$  by  $\lambda_i - 1$  above yields parametrizations for the  $u_v$  and  $d_v$  number densities, needed to compute the valence sum rules. The integral of this number density is finite for  $\lambda_i > 0$ .

We choose a similar parametrization for the antiquark distributions:

$$x\bar{q}_i(x, Q_0^2) = A_i x^{\lambda_{\bar{q}}} (1-x)^{K_{\bar{q}}} \quad \text{for } i = \bar{u}, \bar{d}, \bar{s}, \bar{c}, \bar{b}, \quad (4)$$

where all antiquark flavors have the same  $x$ -dependence but different normalizations. This is acceptable since we are fitting data in a limited large- $x$  range where there is no sensitivity to the different quark flavors. We must have  $-1 < \lambda_{\bar{q}} < 0$  for  $x\bar{q}$  to be integrable and increasing at low  $x$ .

We parameterize the gluon density as the sum of a valence and sea component, with the valence (sea) gluon dominating at large (small) values of  $x$ :

$$\begin{aligned} xg(x, Q_0^2) &= xg^v(x) + xg^s(x) \\ &= A_g^v x^{\lambda_g^v} (1-x)^{K_g^v} + A_g^s x^{\lambda_g^s} (1-x)^{K_g^s} \end{aligned} \quad (5)$$

To obtain an integrable gluon density with a valence (sea) term that decreases (increases) towards low  $x$  we set  $\lambda_g^v > 0$  and  $-1 < \lambda_g^s < 0$ . For the valence component, we keep the power  $K_g^v$  of  $(1-x)$  as a free parameter, while the  $(1-x)$  power of the sea component is set to the  $K_{\bar{q}}$  of the antiquark densities.

This choice of parametrizations yields densities that are positive-definite. Furthermore, the sum rules are easy

and fast to evaluate as Beta functions, and are used to restrict the number of free parameters as follows.

The valence sum rule (2) relates the valence normalizations to the shape parameters by

$$A_i = N_i^v \frac{\Gamma(\lambda_i + K_i + 1)}{\Gamma(\lambda_i)\Gamma(K_i + 1)} \quad i = u, d, \quad (6)$$

with  $N_u^v = 2$  and  $N_d^v = 1$ .

Integrating the valence momentum densities and using the property  $\Gamma(z+1) = z\Gamma(z)$  we find the following relation between the total momentum  $\Delta$  carried by the  $u$  or  $d$  valence quarks and the shape parameters:

$$\Delta_i = N_i^v \frac{\lambda_i}{\lambda_i + K_i + 1} \quad i = u, d \quad (7)$$

which allows us to fix the  $\lambda_i$  by fitting  $\Delta_i$  and  $K_i$ .

Likewise we can fix the normalizations of the antiquark and gluon densities by fitting their momentum fractions  $\Delta$ , subject to the momentum sum rule constraint

$$\Delta_u + \Delta_d + 2 \sum_{\bar{q}} \Delta_{\bar{q}} + \Delta_g^v + \Delta_g^s = 1, \quad (8)$$

where the sum runs over  $\bar{q} = \{\bar{u}, \bar{d}, \bar{s}, \bar{c}, \bar{b}\}$ . The 9 momentum fractions and 7 shape parameters

$$K_u, K_d, \lambda_q, \lambda_g^v, \lambda_g^s, K_{\bar{q}}, \text{ and } K_g$$

give in total 16 parameters to be fitted to the data. Together with the constraint (8) this corresponds to 15 degrees of freedom in the fit.

## PREDICTED NUMBER OF EVENTS

As mentioned above, the parton densities at  $Q_0^2 = 100 \text{ GeV}^2$  were evolved upward at NNLO in the fixed 5-flavor scheme with the program QCDNUM. The strong coupling constant was set to  $\alpha_s = 0.118$  at  $M_Z^2$ .

From the evolved densities the  $F_2$ ,  $F_L$  and  $xF_3$  structure functions were evaluated at NNLO [38–43] and used to compute the neutral current  $e^\pm p$  cross-sections at the Born level. Multiplying by the luminosity of the ZEUS data sets then gives a vector  $\nu$  of binned event expectations.

As described in [16] by the ZEUS collaboration, the vector  $\mathbf{n}$  of expected number of events is calculated from

$$\mathbf{n} = \mathbf{RT} \nu$$

where  $\mathbf{R}$  and  $\mathbf{T}$  are transfer matrices that account for radiative and detector/reconstruction effects, respectively, and map the binning at the Born level to the coarser binning at the observed level. This procedure yields the expected number of events in the 153 bins defined by ZEUS for each data set.

The systematic uncertainties in the ZEUS event reconstruction are given in [16] as deviations from the nominal transfer matrix  $\mathbf{T}$ . The total deviation is then a sum of 10 deviation matrices, weighted by a set of 10 systematic parameters  $\delta_i$  that are left free in the fit.

## PARAMETER EXTRACTION

Assuming that the counts in a bin  $i$  are Poisson distributed with a mean equal to the expected number  $n_i$  of events, we can compute the probability of observing the actual data, given the values of the parameters. Using Bayes' theorem we then calculate the joint posterior probability density of the parameters, given the data, with as input the prior probabilities of the parameters. Single-parameter distributions or correlations among the parameters are evaluated by integrating over the other parameters. The posterior is not only conditional on the data, but also on all the assumptions made in the analysis, such as the choice of parametrizations.

Sound prior knowledge and known physical constraints are easily implemented in the Bayesian approach, but priors should be chosen with care to not introduce unwanted effects in the posterior probability density. Comparing the posterior and prior probability densities provides an easy way to judge the information content of the data.

A 9-dimensional Dirichlet distribution [44] with 9 shape parameters  $\alpha_i$  was chosen for the prior of the momentum components  $\Delta_i$ . Note that a Dirichlet distribution  $\text{Dir}(\boldsymbol{\alpha})$  of  $k$  independent variables  $x_i \in [0, 1]$  lives on a  $(k - 1)$ -dimensional manifold defined by  $\sum x_i = 1$ .<sup>1</sup> With a Dirichlet prior the sum rule (8) is thus automatically satisfied. The choice of the parameters  $\alpha_i$  was guided by the expectation that, asymptotically, gluons and quarks should carry approximately the same momentum, that valence up quarks should carry about twice the momentum of valence down quarks, and that the heavier quarks should carry little momentum.

The parameters  $\alpha_i$  of the Dirichlet distribution are given in Table I, together with the prior distributions of all other parameters. Also listed in the table are the parameter ranges imposed. Note that the  $\lambda$  ranges are set such that all parton distributions are integrable and either vanish, or increase at low  $x$ , as required.

The parameters  $K_u$  and  $K_d$  determine the behavior of the valence quark distributions as  $x \rightarrow 1$ , and their values are of great interest. As given in Table I, we choose as prior a truncated Normal distribution that accommodates a range of about  $K = 3$  to 4 at  $Q^2 = 10 \text{ GeV}^2$ , as found by different global fitting groups [12]. At our

$Q^2$  we expect a somewhat larger value for  $K$  than at  $10 \text{ GeV}^2$ . The Brodsky-Farrar counting rules predict that  $K_{\bar{q}} \approx K_g + 1 \approx K_{u,d} + 2$ . Our priors are set to accommodate this expectation. Note that all our prior choices for the  $K$ -parameters fulfill the requirement that the parton densities, as well as their first derivatives, go to zero as  $x \rightarrow 1$  [12].

The extraction of the parameters of the parton distributions was performed using the Bayesian Analysis Toolkit (BAT.jl) [45]. A Markov Chain Monte Carlo technique was used to sample the posterior probability distribution in the space of the parameters. The accuracy of this data analysis setup was validated using simulated data sets.

A comparison of the measured data to event numbers predicted from the posterior probability distribution is shown in Fig. 1. The predicted counts from the model cover the observed counts well. We evaluated Pearson's  $\chi^2$  for the two data sets using the global mode parameters to evaluate the predicted number of counts, with resulting values of  $\chi^2_P = 322$  from fitting the 306 event numbers. Tests with simulated data yield a  $p$ -value of 0.23, indicating good agreement between the model and the data.

## RESULTS

As discussed in the introduction, the ZEUS high- $x$  data primarily set constraints on the valence distribution of the up quark, and we focus on the relevant parameters here. A summary of the full set of results is given in Table II.

We remind the reader that the parton densities are defined in the  $\overline{\text{MS}}$  scheme at NNLO and parameterized at a scale of  $Q_0^2 = 100 \text{ GeV}^2$ .

Not listed in Table II are the parameters  $\Delta_{\bar{s},\bar{c},\bar{b}}$ ,  $\lambda_g^v$  and  $\lambda_g^s$  since no significant reduction of the prior range was observed in the posterior. We find 68 % probability

TABLE I. Priors used in the parton density fit for all parameters. There are 9 parameters in the vector  $\boldsymbol{\alpha}$  and 10 in  $\boldsymbol{\delta}$ . The normal distributions are truncated to the range indicated and their mean and sigma are given in brackets.

	Prior	Range
$\boldsymbol{\alpha}$	Dir(20, 10, 20, 20, 5, 2.5, 1.5, 1.5, 0.5)	[0, 1]
$K_u$	Normal(3.5, 0.5)	[2, 5]
$K_d$	Normal(3.5, 0.5)	[2, 5]
$\lambda_g^v$	Uniform	[0, 1]
$\lambda_g^s$	Uniform	[-1, -0.1]
$K_g$	Normal(4, 1.5)	[2, 7]
$\lambda_{\bar{q}}$	Uniform	[-1, -0.1]
$K_{\bar{q}}$	Normal(4, 1.5)	[3, 10]
$\boldsymbol{\delta}$	Normal(0, 1)	[-5, 5]

<sup>1</sup> A Dirichlet distribution is a multivariate generalization of the Beta distribution. For instance  $\text{Beta}(\alpha_1, \alpha_2)$  of one variable  $x$  is the same as  $\text{Dir}(\alpha_1, \alpha_2)$  of two variables  $(x_1, x_2)$  with  $x_1 + x_2 = 1$ .

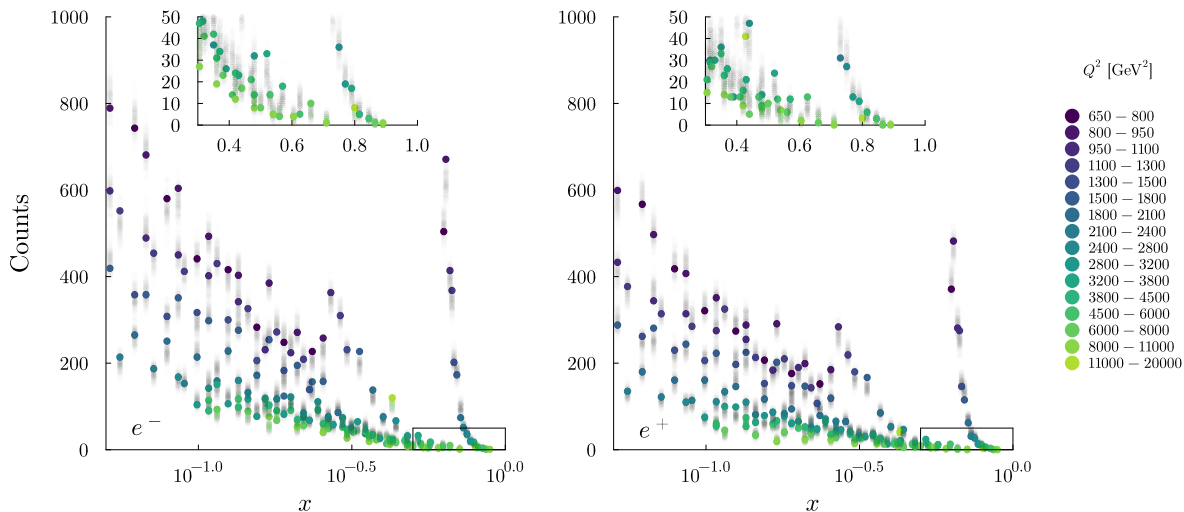


FIG. 1. Predictions of event numbers calculated from sampling the posterior probability distribution of the fitted parameters (shaded bands) compared to the ZEUS data (filled dots) for  $e^-p$  (left) and  $e^+p$  scattering (right). The predictions and data are displayed at the center of the bins in which events are recorded. For clarity the boxes at large  $x$  are shown enlarged in the insets.

upper limits  $2\Delta_{\bar{s}} < 0.027$ ,  $2\Delta_{\bar{c}} < 0.038$  and  $2\Delta_{\bar{b}} < 0.007$ . The prior ranges of  $\lambda_g^v$  and  $\lambda_g^s$  are given in Table I.

Figure 2 shows a comparison of the prior and posterior probability contours for  $K_u$  and  $\Delta_u$  as well as their marginal distributions. As is clear in the figure, the data strongly constrains these parameters. The momentum fraction carried by the valence up quark distribution was found to be  $\Delta_u \approx 0.22$  with a credible interval of  $\{0.210-0.228\}$  where, unless otherwise stated, we will in the following always refer to the smallest intervals with 68% probability content. Such a high precision measurement of  $\Delta_u$  has, to the best of our knowledge, not yet been reported in the literature.

We obtained for the power of the up-valence ( $1-x$ ) component a value of  $K_u \approx 3.8$  with a credible interval

of  $\{3.61-3.92\}$ . We subdivided the data into a set of bins containing data with  $x \geq 0.5$  and the complement. The resulting intervals were  $\{3.40-4.03\}$  ( $\{3.71-4.52\}$ ) for the lower- (higher-)  $x$  data, indicating that the higher- $x$  data indeed provide valuable new information.

The summary of previously measured  $K_u$  values in [12]

TABLE II. Parameter values obtained from this analysis. For each parameter is given the value of the mode of the joint posterior and of its marginal distribution, with errors corresponding to the 68% smallest credible interval. The fit does not constrain the values of  $\Delta_{\bar{s},\bar{c},\bar{b}}$ ,  $\lambda_g^v$  and  $\lambda_g^s$  (see text).

	Global mode	Marginal mode		Global mode	Marginal mode
$\Delta_u$	0.225	$0.219_{-0.009}^{+0.009}$	$K_u$	3.89	$3.74_{-0.13}^{+0.18}$
$\Delta_d$	0.084	$0.092_{-0.026}^{+0.023}$	$K_d$	3.18	$3.51_{-0.42}^{+0.53}$
$\lambda_{\bar{q}}$	-0.50	$-0.54_{-0.09}^{+0.09}$	$K_{\bar{q}}$	7.42	$6.38_{-1.42}^{+1.17}$
$K_g$	4.69	$5.02_{-1.21}^{+1.21}$			
$2\Delta_{\bar{u}}$	0.092	$0.100_{-0.024}^{+0.026}$	$2\Delta_{\bar{d}}$	0.032	$0.022_{-0.014}^{+0.022}$
$\Delta_g^v$	0.250	$0.245_{-0.044}^{+0.040}$	$\Delta_g^s$	0.275	$0.251_{-0.045}^{+0.040}$

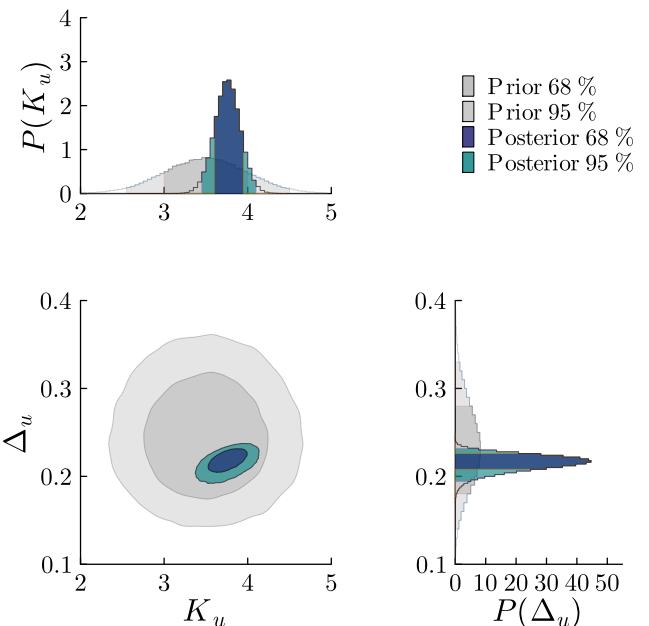


FIG. 2. Joint probability contours of the up-valence parameters  $K_u$  and  $\Delta_u$  (lower left) and the marginal distributions of  $K_u$  (top) and  $\Delta_u$  (lower right). Shown are the 68 and 95% smallest credible intervals for both the prior (light shaded) and posterior (dark shaded) distributions.

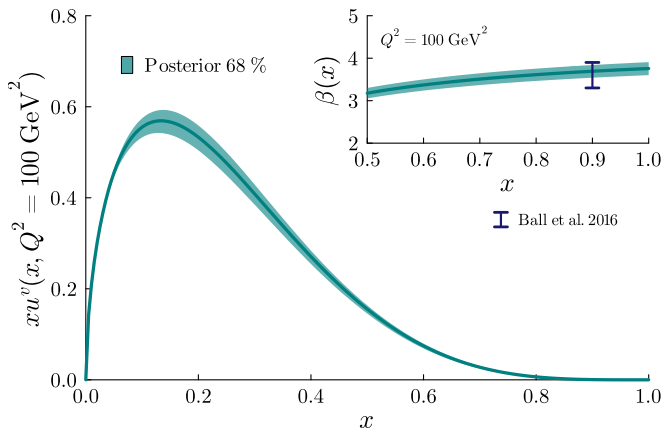


FIG. 3. The valence distribution  $xu^v$  and the effective  $(1-x)$  power  $\beta$  from this analysis at a value of  $Q^2 = 100 \text{ GeV}^2$ . The 68% smallest probability contour is depicted. The vertical range plotted in the inset summarizes the results on  $\beta$  reported in [12].

includes results with stricter bounds than reported here. However, these were determined from data at much lower  $Q^2$  where higher-twist effects may play a role, and which do not extend to the highest values of  $x$ , as do the present data. Furthermore in [16] it is shown that different high- $x$  parton distributions do not overlap within their quoted uncertainties.

We follow the suggestion given in [12] and calculate the effective power of  $(1-x)$ :

$$\beta(x, Q_0^2) = \frac{\partial \ln[xu^v(x, Q_0^2)]}{\partial \ln(1-x)} \quad (9)$$

and show the result in Fig. 3 where we also compare our results to a summary of  $\beta$ -values at  $x = 0.9$  reported in [12]. Our analysis agrees well with these results, and provides a more constrained range of values. It should be noted, however, that our result for  $\beta(x)$  is not only constrained by the data, but possibly also by the form of the parametrization chosen and that such a parametrization dependence is left for investigation in a future analysis.

Figure 3 also shows our result on the  $xu^v$  distribution. Although plotted down to a value of  $x = 0$ , we remind the reader that our parametrizations are not meant to describe the parton densities at very small values of  $x$ , as we have only analyzed data in the range  $x > 0.03$ .

Using (7) to compute  $\lambda_u$  from  $\Delta_u$  and  $K_u$  gives a value of  $\lambda_u \approx 0.58$  with a credible interval of  $\{0.53-0.62\}$ .

For the momentum fractions besides that of the valence up-quark, we obtain

$$\begin{aligned} \Delta_d &\approx 0.11 && \{0.07-0.12\} \\ \Delta_{\text{sea}} = 2 \sum_{\bar{q}} \Delta_{\bar{q}} &\approx 0.17 && \{0.16-0.22\} \\ \Delta_g = \Delta_g^v + \Delta_g^s &\approx 0.50 && \{0.47-0.53\}. \end{aligned}$$

With the fitted data, there is little sensitivity to the gluon

density and the approximately equal momentum sharing between the quarks and gluons is largely a consequence of our prior choice on  $\Delta_g$ .

The  $(1-x)$  powers for the valence down-quark and the gluon were found to be  $K_d \approx 3.5$  and  $K_g \approx 5.0$  with credible intervals  $\{3.1-4.0\}$  and  $\{3.8-6.2\}$ , respectively. The sea densities had a power of  $(1-x)$  of  $K_{\bar{q}} \approx 6.4$  with credible interval  $\{5.0-7.6\}$ . These values are in line with the expectation that  $K_d \approx K_u$  and that  $K_g > K_{u,d}$  and  $K_{\bar{q}} > K_g$ .

## SUMMARY

We have performed the first analysis of the ZEUS high- $x$  data set [15] and extracted precise information on the momentum content and  $x$  dependence of the valence up-quark distribution at the highest values of  $x$ . The analysis was based on a forward modeling approach, taking parton distributions at a scale of  $Q_0^2 = 100 \text{ GeV}^2$  and evolving them upward with the QCDNUM program at NNLO in QCD perturbation theory. The evolved parton distributions were then used to predict expected event numbers in the measurement intervals used by the ZEUS Collaboration, and a Poisson probability was evaluated for the individual measurements. The full posterior probability distribution of the parameters of parton distributions was then evaluated in a Bayesian fit using the BAT.jl package. All systematic uncertainties associated with the data were included in this analysis.

The high- $x$  data from ZEUS primarily inform us on the valence up-quark distribution. Given our simple parametrizations, which are adequate for the data analyzed, we obtain a precision of 1% on the total momentum carried by the up-valence quarks, while the power of  $(1-x)$  was found to be in the range  $3.6 - 3.9$  at  $Q^2 = 100 \text{ GeV}^2$ . These results, based on data at the highest values of  $x$ , represent a significant step in our understanding of the proton.

## ACKNOWLEDGMENTS

The authors thank Andrii Verbytskyi for his help in the technical developments of the PartonDensity.jl package, as well as Amanda Cooper-Sarkar, Pavel Nadolsky and Aurore Courtoy for informative discussions. We are especially grateful to I. Abt for her help in identifying an error in our data set selection in an earlier version of this manuscript. We thank T. Rogers for his comment on the positivity requirement of  $\overline{MS}$  parton densities. R. Aggarwal acknowledges the support of Savitribai Phule Pune University. F. Capel was employed by the Excellence Cluster ORIGINS, which is funded by the Deutsche Forschungsgemeinschaft (DFG, German Research Foundation) under Germany's Excellence Strategy - EXC-2094-390783311, during much of the project duration.

- 
- \* ritu.aggarwall@gmail.com  
† m.botje@nikhef.nl  
‡ caldwell@mpp.mpg.de  
§ capel@mpp.mpg.de  
¶ oschulz@mpp.mpg.de
- [1] T. Cridge, L. A. Harland-Lang, A. D. Martin, and R. S. Thorne, *Eur. Phys. J. C* **82**, 90 (2022).  
[2] S. Bailey, T. Cridge, L. A. Harland-Lang, A. D. Martin, and R. S. Thorne, *Eur. Phys. J. C* **81**, 341 (2021).  
[3] T.-J. Hou *et al.*, *Phys. Rev. D* **103**, 014013 (2021).  
[4] S. Dulat *et al.*, *Phys. Rev. D* **93**, 033006 (2016).  
[5] S. Alekhin *et al.*, *Eur. Phys. J. C* **78**, 477 (2018).  
[6] S. Alekhin *et al.*, *Phys. Rev. D* **89**, 054028 (2014).  
[7] R. D. Ball and others [NNPDF Collaboration], *Eur. Phys. J. C* **82**, 428 (2022).  
[8] R. D. Ball and others [NNPDF Collaboration], *Eur. Phys. J. C* **77**, 663 (2017).  
[9] I. Abt *et al.* (H1 and ZEUS Collaborations), *Eur. Phys. J. C* **82**, 243 (2022).  
[10] H. Abramowicz *et al.* (H1 and ZEUS Collaborations), *Eur. Phys. J. C* **75**, 580 (2015).  
[11] M. Constantinou *et al.*, *Prog. Part. Nucl. Phys.* **121**, 103908 (2021), arXiv:2006.08636 [hep-ph].  
[12] R. Ball, E. Nocera, and J. Rojo, *Eur. Phys. J. C* **76**, 383 (2016).  
[13] A. Courtoy and P. M. Nadolsky, *Phys. Rev. D* **103**, 054029 (2021), arXiv:2011.10078 [hep-ph].  
[14] S. J. Brodsky and G. R. Farrar, *Phys. Rev. Lett.* **31**, 1153 (1973).  
[15] H. Abramowicz *et al.* (ZEUS Collaboration), *Phys. Rev. D* **89**, 072007 (2014).  
[16] I. Abt *et al.* (ZEUS Collaboration), *Phys. Rev. D* **101**, 112009 (2020).  
[17] V. N. Gribov and L. N. Lipatov, *Sov. J. Nucl. Phys.* **15**, 438 (1972).  
[18] V. N. Gribov and L. N. Lipatov, *Sov. J. Nucl. Phys.* **15**, 675 (1972).  
[19] L. N. Lipatov, *Sov. J. Nucl. Phys.* **20**, 94 (1975).  
[20] Y. L. Dokshitzer, *Sov. Phys. JETP* **46**, 641 (1977).  
[21] G. Altarelli and G. Parisi, *Nucl. Phys. B* **126**, 298 (1977).  
[22] J. Butterworth *et al.*, *J. Phys. G: Nucl. Part. Phys.* **43**, 023001 (2016).  
[23] J. Rojo *et al.*, *J. Phys. G: Nucl. Part. Phys.* **42**, 103103 (2015).  
[24] R. D. Ball *et al.*, (2022), arXiv:2203.05506 [hep-ph].  
[25] *A description of the technical developments carried out during this project is in preparation.*  
[26] F. Halzen and A. D. Martin, *Quarks and Leptons: an introductory course in modern particle physics* (1984).  
[27] M. Botje, *Comput. Phys. Commun.* **182**, 490 (2011), arXiv:1005.1481 [hep-ph].  
[28] O. V. Tarasov, A. A. Vladimirov, and A. Y. Zharkov, *Phys. Lett. B* **93**, 429 (1980).  
[29] G. Curci, W. Furmanski, and R. Petronzio, *Nucl. Phys. B* **175**, 27 (1980).  
[30] W. Furmanski and R. Petronzio, *Phys. Lett. B* **97**, 437 (1980).  
[31] W. Furmanski and R. Petronzio, *Z. Phys. C* **11**, 293 (1982).  
[32] S. A. Larin and J. A. M. Vermaseren, *Phys. Lett. B* **303**, 334 (1993), arXiv:hep-ph/9302208.  
[33] K. G. Chetyrkin, B. A. Kniehl, and M. Steinhauser, *Phys. Rev. Lett.* **79**, 2184 (1997), arXiv:hep-ph/9706430.  
[34] M. Buza, Y. Matiounine, J. Smith, and W. L. van Neerven, *Eur. Phys. J. C* **1**, 301 (1998), arXiv:hep-ph/9612398.  
[35] S. Moch, J. A. M. Vermaseren, and A. Vogt, *Nucl. Phys. B* **688**, 101 (2004), arXiv:hep-ph/0403192.  
[36] A. Vogt, S. Moch, and J. A. M. Vermaseren, *Nucl. Phys. B* **691**, 129 (2004), arXiv:hep-ph/0404111.  
[37] R. D. Ball, V. Bertone, M. Bonvini, S. Forte, P. Groth Merrild, J. Rojo, and L. Rottoli, *Phys. Lett. B* **754**, 49 (2016), arXiv:1510.00009 [hep-ph].  
[38] J. Sanchez Guillen, J. Miramontes, M. Miramontes, G. Parente, and O. A. Sampayo, *Nucl. Phys. B* **353**, 337 (1991).  
[39] W. L. van Neerven and E. B. Zijlstra, *Phys. Lett. B* **272**, 127 (1991).  
[40] E. B. Zijlstra and W. L. van Neerven, *Phys. Lett. B* **273**, 476 (1991).  
[41] E. B. Zijlstra and W. L. van Neerven, *Phys. Lett. B* **297**, 377 (1992).  
[42] W. L. van Neerven and A. Vogt, *Nucl. Phys. B* **568**, 263 (2000), arXiv:hep-ph/9907472.  
[43] W. L. van Neerven and A. Vogt, *Nucl. Phys. B* **588**, 345 (2000), arXiv:hep-ph/0006154.  
[44] M. Betancourt, *AIP Conference Proceedings* **1443**, 157 (2012).  
[45] O. Schulz, F. Beaujean, A. Caldwell, C. Grunwald, V. Hafych, K. Kröniger, S. L. Cagnina, L. Röhrig, and L. Shtembari, *SN Computer Science* **2**, 210 (2021).